SPATIO-TEMPORAL EVOLUTION OF SODIUM AEROSOL AND TEMPERATURE DISTRIBUTION DURING SODIUM POOL FIRE IN A CONFINED ENVIRONMENT

AMIT KUMAR[1], USHA PUJALA[1], E. HEMANTH RAO[2], G. VENKAT REDDY[3], V. SUBRAMANIAN[1], SANJAY KUMAR DAS[3], D. PONRAJU[2], S. ATHMALINGAM[3], B. VENKATRAMAN[1]

[1]Radiological and Environmental Safety Group, Indira Gandhi Center for Atomic Research, A CI of Homi Bhabha National Institute, Kalpakkam - 603102, India.
[2]Health, Safety and Engineering Group, Indira Gandhi Center for Atomic Research, A CI of Homi Bhabha National Institute, Kalpakkam - 603102, India.
[3]Health, Safety and Engineering Group, Indira Gandhi Center for Atomic Research, Kalpakkam - 603102, India.

Email contact of the corresponding author: amitpatel@igcar.gov.in (Dr. Amit Kumar)

Abstract

In case of a Core Disruptive Accident in sodium-cooled fast reactor, sodium will be ejected from the reactor vessel into the Reactor Containment Building (RCB) and results in sodium fire. Liquid sodium combustion generates aerosol, which gets dispersed and remains suspended in RCB based on geometry of the building and degree of turbulence. The Environment Source Term (EST) primarily depends on the dynamics of sodium aerosols inside the containment. Hence, it is essential to carry out a safety analysis of SFR using computational tools and models shall be validated with experimental data, particularly aerosol dynamics inside the containment along with thermal hydraulics. Besides, all codes assume uniform aerosol concentration in large containment buildings and the evolution of suspended concentration was predicted. However, in actual case a non-uniform concentration profile exists, which leads to stratification of aerosol concentration inside the containment. Towards assessment of aerosol dynamics in realistic scenario, spatial-temporal characteristics of sodium aerosol and temperature distribution were studied by conducting sodium pool fire experiments in a large containment.

The sodium fire experiment was conducted by using ~ 2.0 kg of sodium in a pool area of ~ 0.25 m^2. The measured maximum pool and gas temperatures are 685 ºC and 126 °C respectively, and the temperature gradient at the wall boundary layer was 7.5 °C/cm. The estimated average sodium burning rate and aerosol release rate are 17.3 kg/m^2hr and 0.24 g/s, respectively. The spatial variation of aerosol characteristics was measured for both horizontal and vertical planes. The measured maximum aerosol concentration in the horizontal plane ranges from 2.76 – 5.32, 2.16 – 3.30 and 2.09 – 4.21 g/m^3 for the bottom, middle and top elevations respectively. For the vertical plane, aerosol concentration varied from 2.16 – 3.65 g/m^3 for central positions and 2.53 – 5.32 g/m^3 for off-center positions. The trend of average suspended aerosol concentration at each elevation showed that the concentration was higher at the top elevation than at the middle and bottom for up to 15 minutes i.e., during aerosol generation period and after that concentration was found to be higher at the bottom elevation for the next 25 minutes. Based on the measurements, it is observed that the aerosol distribution is not well mixed within the experimental period. A significant difference in aerosol mass concentration was observed between each elevation, between estimation and observations based on a zero-dimensional model. The evolutions of aerosol median size by theoretical simulation capture the overall trend reasonably.

1. INTRODUCTION

Towards safety analysis of Sodium cooled Fast Reactors (SFR), activity release fraction from core to reactor containment building (RCB), i.e., in-containment source and the environment source term (EST), i.e., RCB to the environment are essential topics for both designers and regulators. The in-containment source depends on the release fraction of core inventory to RCB, radioactive decay and aerosol dynamics inside RCB [1]. The aerosol dynamics in the containment is very complex due to the mixed behaviour of aerosols released from sodium combustion, fuel, and fission products as well as various aerosol natural processes (i.e., different agglomerations, gravitational settling, diffusion, thermophoretic and turbulence deposition etc.). Since the sodium combustion reactions are exothermic in nature, the temperature and pressure in the containment are expected to rise. Further, the reaction products (Na_2O and Na_2O_2) start to nucleate and condense, leading to formation of sodium aerosols and at the same time, the oxides aerosol reacts with moisture and converted to the hydroxide instantaneously (~

millisecond). The hydroxide aerosol gets converted to sodium carbonate upon reaction with CO_2 then it further converts to bicarbonate. The reaction rate of sodium carbonate and bicarbonate is relatively slow than hydroxide and depends on many parameters like, moisture, aerosol concentration and CO_2 concentration. The fission product vapours condense to form particulate and interact with sodium combustion aerosol. The aerosol gets dispersed and remains suspended in the containment according to the geometry of the building, degree of turbulence and until they settle down or leaked. The EST depends on (i) the concentration of the aerosols remains suspended (available for release) in the containment as a function of time following the postulated accident [2], and (ii) the leakage rate from the containment stack, ducts, and cracks of RCB. The evolution of aerosol concentration inside the containment and deposition on the walls and floor of the containment is crucial for predicting EST. Hence, it is of utmost importance to conduct a safety analysis of SFRs, and the deployed numerical models, shall be validated with good experimental observations, particularly aerosol dynamics inside the containment and thermal hydraulics.

In the past, many experiments were done on various scales of test facilities like Aerosol Test Facility (ATF – volume: 1 m^3) India [3, 4], MISUBUSHI Facility (volume: 21 m^3) Japan [5], FAUNA Test Facility (volume: 220 m^3) Germany [6], CSTF Vessel (volume: 850 m^3) Washington, USA [7], DFBR Facility (volume: 2600 m^3), Japan [8] and ESMERALDA Test Facility (volume: 3600 m^3) France [9]. The dimension of facilities varies three orders in volume. From the above works, it is observed that the formation and characterization of sodium aerosol are well described. The theoretical calculation for predicting aerosol transport and deposition within the containment following severe accident conditions is well explained. Several theoretical codes have been developed for predicting particle size distribution, the evolution of concentration, and various depositions phenomena and agglomerations. The codes like CONTAIN, PARDISEKO IIIb [10], HAA-3B [11], ASTEC-Na [12, 13] and HAARM [14] etc assume and simulate uniform aerosol characteristics (concentration, size, chemical species, and deposition velocity etc.) in the containment volume. This assumption may hold good for small-scale experimental facilities (ATF and MISUBUSHI); however, this may not be true for large containments where aerosol have a non-uniform distribution followed by stratified aerosol deposition on the floor. Hence, the foremost requirement is the continued development of codes toward realistic estimation of EST for which no unequivocal experimental evidence is available. The development of codes may need to handle non-uniform aerosol concentration within the containment volume and the radiological impact on aerosols due to the prevailing radiation field. Towards that, a realistic experimental data remains necessary in measuring the non-uniform concentration profile of a given containment volume for a specific source generation data (rate and duration of aerosol generation). Following the experimental works, an aerosol dynamic coupled with the fluid dynamics-based computational model is to be developed for predicting the non-uniform distribution of aerosols in the containment by taking the input from aerosol source, and thermal-hydraulics data. Further, the evolution of suspended aerosol concentration should be determined under non-uniform distribution and shall be modelled based on the aerosol dynamic model considering all aerosol processes.

Radiological and Environmental Safety Division (RESD), Indira Gandhi Centre for Atomic Research (IGCAR) is involved in assessing source terms to the containment as a part of radiological safety studies under severe accident conditions of SFRs. In the present work, the spatial-temporal characteristics of sodium aerosol and temperature distribution were studied by conducting sodium pool fire experiments using ~ 2.0 kg of sodium in a pool area of ~ 0.25 m^2 in a sodium fire facility (MINA). The facility consists of a rectangular steel test chamber of 150 m^3 volume and real time off-line aerosol metrological devices, sodium system, instrumentation, convection flow, pressure sensor, an array of thermocouples for spatial-temporal temperature monitoring along with data acquisition and a high-speed video imaging system. The aerosol behaviour in the test chamber was monitored in 12 locations at three elevations with real-time and offline aerosol metrological devices. The multi elevation aerosol sampling was done for observation of stratification in aerosol concentration. The spatiotemporal temperature evolution was obtained for the sodium pool, above the pool region, inside the chamber at various locations and near the chamber wall by using ~ 40 thermocouples. The relative humidity was also monitored during the experiment.

The aim of the current work is to produce representative experimental data allowing access to the evolution of spatial-temporal characteristics of sodium aerosol concentration and size distribution produced inside a closed enclosure. A zero-dimensional numerical model was applied for evolution of aerosol concentration and compared with measured concentration values. The article is structured as follows: Section 2 discusses the details of the experimental facility, sampling layout and details of various aerosol metrological devices. Section 3 gives a brief

description of the results, analysis of the experiment and compares the observation with theoretical estimations. Section 4 concludes the findings.

2. MATERIAL AND METHODS

The experimental study in the present work is conducted in Mini Sodium fire facility (MINA), Safety Engineering division (SED). The facility is meant for conducting experiments on sodium fires (pool and spray) to investigate consequences such as temperature, pressure build-up, and aerosol behaviour in an enclosed chamber simulating to the RCB.

2.1. Experimental facility

The schematic of the MINA facility is shown in Fig. 1. The facility consists of a closed rectangular steel test chamber of size 6.0 m x 5.45 m x 4.6 m with a volume of 150 m^3 [15] and designed to withstand an internal pressure of 1 bar at 300 ºC. The test chamber is provided with a leak-tight door of 2.0 m x 1.5 m, an SS liner on the inner wall and a control room located outside the chamber. The facility has a dedicated sodium supply system, instrumentation and control room as shown in Fig.1. The test chamber is mounted with state-of-the-art equipment and instruments to monitor dynamic pressure, spatial gas, and wall temperature distribution, data acquisition, and two viewing ports for the high-speed video and thermal imaging system.

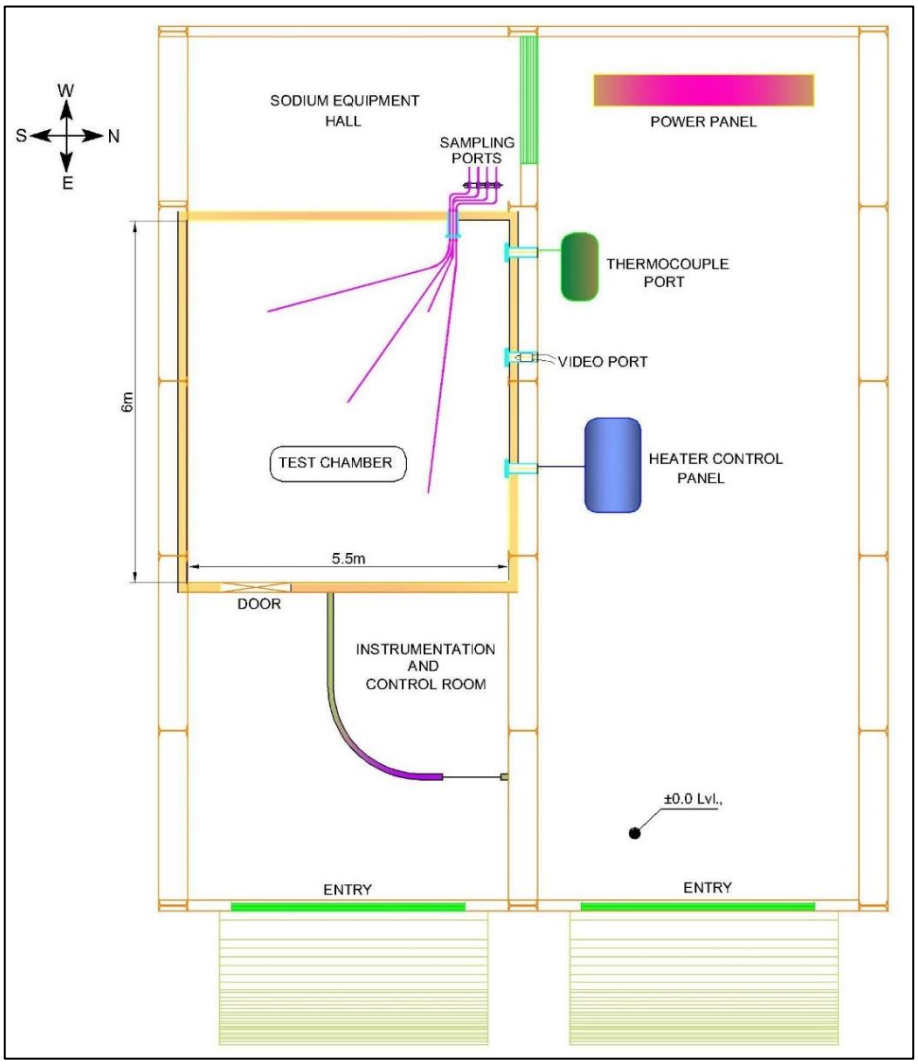

FIG. 1. The layout of the MINA experimental facility.

2.2. Sodium aerosol generation by a pool fire

The experimental setup for sodium pool fire consists of an SS tray of 0.5 m x 0.5 m x 0.05 m, a sodium supply tank and argon supply system as shown in Fig. 2. The tray is meant to create a sodium pool fire is positioned on floor at centre of the test chamber. Both the tray and sodium supply tank were provided with surface heaters. The sodium supply tank was loaded with about 2.1 kg of pure sodium and argon cover gas was maintained at a pressure of 0.05 bar above atmosphere. The tray and sodium supply tank were heated to 350 ± 2.63 ºC by using surface heaters while maintaining the argon pressure in the vessel at ~ 0.05 bar. Liquid sodium was drained from the supply tank to the tray by pressurizing the sodium tank with argon at 0.2 bar. As the tray was maintained at 350 ± 2.63 ºC, released sodium resulted in a pool fire, leading to sodium aerosol generation.

FIG. 2. Optical image of sodium supply tank and tray for pool fire.

2.3. Sampling layout inside the experimental hall

The experiment was carried out by burning ~ 2.0 kg of sodium in pool mode. Sodium combustion aerosol was sampled in 12 locations at three elevations viz. 1.2, 3.0 and 3.85 m from the chamber floor and four azimuthal locations on each elevation to obtain the spatial distribution of aerosol. Each sampling location was connected through an SS tube of 10 mm internal diameter. The length of the sampling line was restricted to less than 5 m to minimize the aerosol deposition in the sampling line. Each sampling line consists of a ball valve and the necessary aerosol sampling device. The three-dimensional isometric view of the sampling positions and temperature monitoring locations are shown in Fig.3 and their positions are listed in Table 1.

TABLE 1. THE CONFIGURATION OF THE SPATIAL AEROSOL SAMPLING POSITIONS

S. N.	Sample notation	Height (m)	Location (length x width)	Sampling zone
1.	Centre (CT)	3.85	3.1 x 2.75	Top
2.	South–West (SWT)	3.85	4.60 x 1.25	Top
3.	North–West (NWT)	3.85	4.60 x 4.25	Top
4.	North- East (NET)	3.85	1.60 x 4.25	Top
5.	Centre (CM)	3.0	3.1 x 2.75	Middle
6.	South–West (SWM)	3.0	4.60 x 1.25	Middle
7.	North–West (NWM)	3.0	4.60 x 4.25	Middle
8.	North- East (NEM)	3.0	1.60 x 4.25	Middle
9.	Centre (CB)	1.2	3.1 x 2.75	Bottom
10.	South–West (SWB)	1.2	4.60 x 1.25	Bottom
11.	North–West (NWB)	1.2	4.60 x 4.25	Bottom
12.	North- East (NEB)	1.2	1.60 x 4.25	Bottom

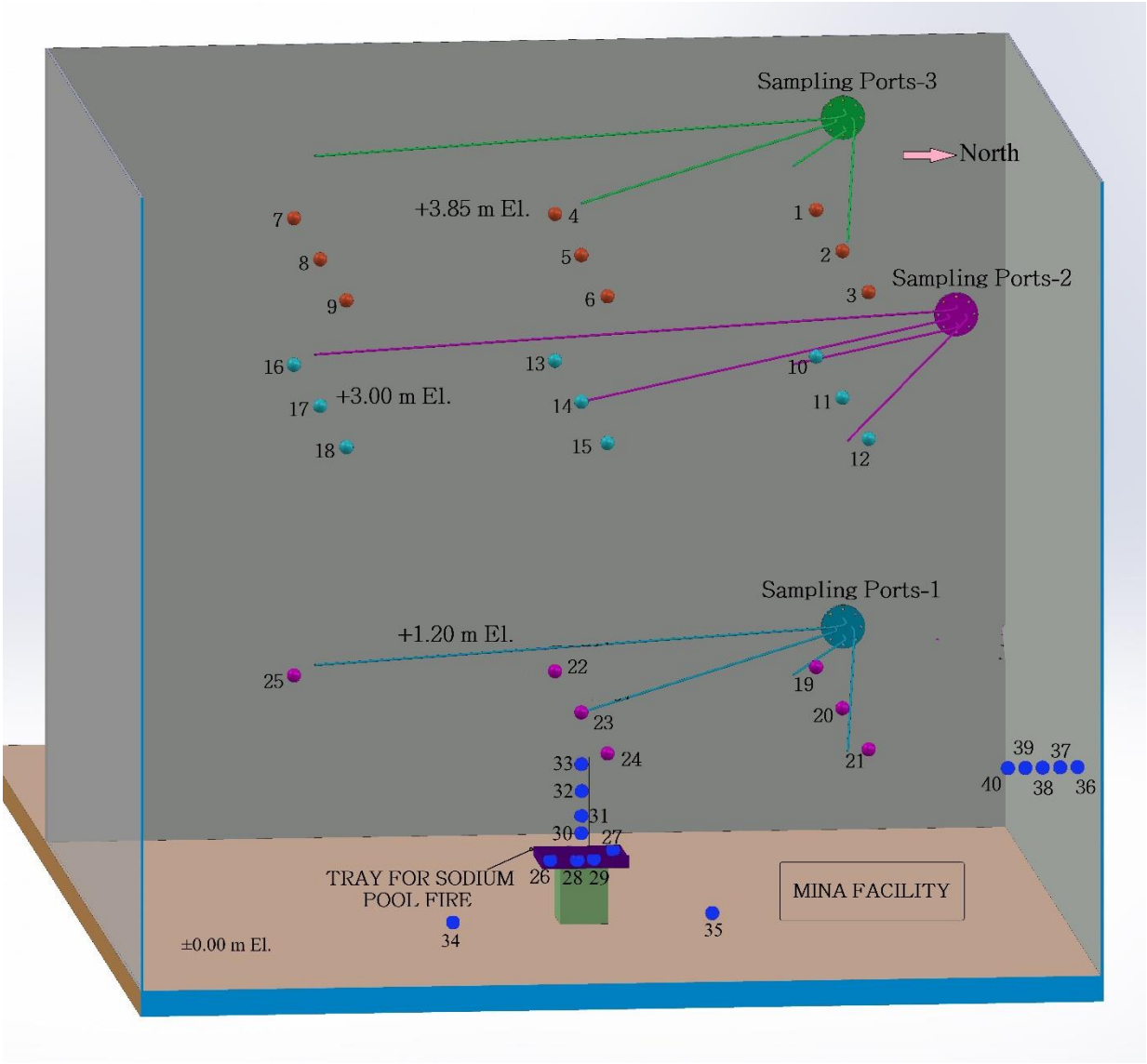

FIG. 3. Three-dimensional isometric view of aerosol sampling locations and temperature measuring locations.

2.4. Aerosol metrological devices

To study a wide range of aerosol characteristics, both off-line and real-time sampling techniques were employed. The spatiotemporal characteristics of aerosols have been sampled at three elevations of the chamber using aerosol diagnostic instruments like Filter Paper Sampler (FPS), Low-Pressure Impactor (LPI), and aerosol spectrometer (Model: 1.108 and Make: GRIMM Aerosol Technik, Germany). The list of equipment used, their principle of operation and measuring characteristics and range are summarized in Table 2. A detailed description of equipment and methods, their operation and working principle can be found in an earlier paper [16]. Turntable equipment is used to determine aerosol mass flux and deposition velocities. The instrument is designed and fabricated indigenously [17]. It consists of a circular top plate and a circular collection plate. The collection plate is connected beneath the top plate on a central axis and provided with 16 slots of 25 mm diameter, on which pre-weighed glass plates were mounted. The top plate has got only one opening for the entry of aerosols in such a way that it is aligned in the same vertical line with one of the 16 slots of the collection plate. The collection plate is rotated and aligned to the next slot by using a stepper motor and controller. The controller unit is provided with an automatic timer circuit for the rotation of the collection plate. The SS plates of 100 cm^2 (10 cm x 10 cm) were placed on the floor and pasted on the sidewall and downward-facing surface of the chamber to collect cumulative aerosol deposition mass.

TABLE 2. AEROSOL METROLOGICAL DEVICES, OPERATING PRINCIPLE AND MEASURING RANGE

Instrument	Principle	Measured Characteristics	Measuring Range	On-line/ Off-line
Filter paper sampler	Gravimetric + chemical	Mass concentration	--	Off-line
Low-Pressure Impactor	Impaction + Gravimetric	Mass-size distribution	0.08 - 35 µm	Off-line
Aerosol Spectrometer	Light Scattering	Number/ mass-size distribution	0.3 – 20 µm	On-line
Turn Table Technique	Mass deposit	Deposition flux/ velocity	--	Off-line
SS collection plates	Chemical	Aerosol fallout	--	Off-line

2.5. Matrix for temperature monitoring inside the test chamber

The temperature distribution in the sodium pool, gas, and test chamber wall was measured using a matrix of K-type thermocouples (40 Nos.) with a range of -200 ºC to 1300 ºC, with an accuracy ± 0.75% of the measured value. Each thermocouple was connected to a data acquisition system for recording the data at a time interval of 0.5 seconds. Twenty-five thermocouples were positioned in space at three elevations (9 in the top and middle and 7 in the bottom elevation) for gas temperature monitoring. One thermocouple is placed at the centre of the chamber at each elevation. In the top and middle elevation, four sensors are located at a 1.5-meter distance from the centre to each side and the remaining four are diagonally positioned from the centre at ~ 2 meters. In the bottom elevation, the sensor position was the same as the middle and top, except for two sensors were not placed because of the hindrance due to the door. The temperatures in the sodium pool and air above the surface were monitored by using eight thermocouples. The SS tray was also provided with four thermocouples on the surface of the tray and four thermocouples were placed at different heights (50, 100, 200 and 300 mm above the tray surface) for monitoring gas temperatures above the burning sodium. Two thermocouples were mounted on the floor to monitor the surface temperature. The temperature gradient near the chamber wall was measured using five thermocouples spaced equally by 2 mm. Relative humidity sensors with a range of 0 – 100 % with ± 0.8 % accuracy were also provided in the test chamber to monitor relative humidity during the experiments.

3. RESULTS AND DISCUSSION

3.1. Sodium combustion and aerosols generation

The 2 kg sodium was drained into the tray in ~ 15 s. As soon as the liquid sodium is drained into the hot SS tray from the sodium supply tank, a sodium pool was formed and burning started instantaneously. The sodium burning scenario was recorded using a high-speed optical camera and the images are shown in Fig.4 (A – H). Visual images show the upward movement of aerosol inside the chamber at the initial phase of combustion due to a strong thermal gradient in the vertical direction. During the sodium combustion, dense white smoke was generated and observed to spread throughout the chamber (D - E). With a gradual reduction in visibility was observed due to the increase in aerosol concentrations inside the chamber (F - H). The visibility was entirely lost in ~ 15 min from the start of the experiment (H). Based on the optical observation, the total burning time could not be accurately estimated.

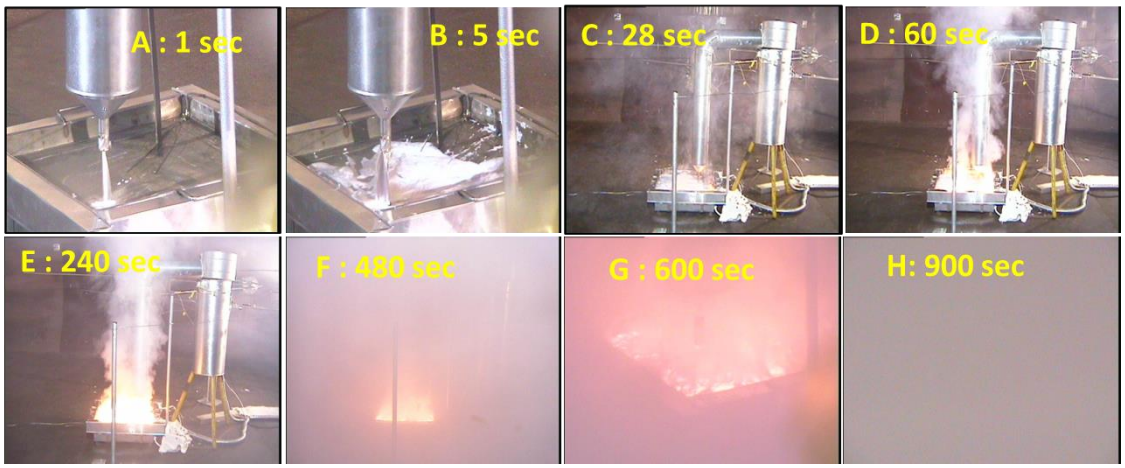

FIG. 4. Optical images of sodium draining from the vessel and pool burning.

3.2. Temperature distribution inside the experimental hall

The rise in temperature due to the heat evolved during sodium fire near the sodium pool surface is shown in Fig.5. After the liquid sodium drained at T_0 (1430 s), sodium fire occurred instantaneously upon draining due to rapid oxidation and reaction with moisture. The rise in pool temperature started as soon as the sodium was exposed to the collection tray, but the rising rate was slow owing to the continuous collection of sodium into the tray. Then the temperature was observed to increase slowly up to 280 ± 2.1 ºC in 5-min (from T_0). Sodium pool temperature in the tray was raised to a maximum of 685 ± 5.2 ºC in ~ 10 minutes and remained at ~ 660 ± 5.0 ºC until the completion of sodium combustion (~25 minutes from the T_0). Later, a gradual decrease in temperature was observed. In about 2 hours, the temperature of the sodium pool decreased to less than 150 ± 1.1 ºC. The floor temperature of the chamber was observed to increase to 43 ± 0.3 ºC from 30 ± 0.2 ºC during the combustion phase and reduced after the combustion. Temperature near the sodium pool surface was ~ 550 ± 4.1 ºC (at 50 mm above the collection tray) and decreased with vertical distance. The temperature at 0.3 m away from the pool was ~ 200 ± 1.5 ºC only.

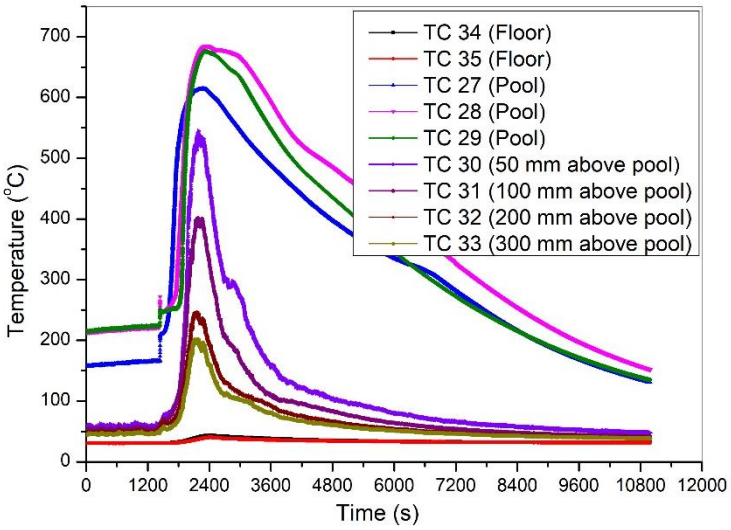

Fig. 5. Evolution of temperature during sodium pool fire.

The temperature distributions at the different elevations and near the chamber wall are shown in Fig. 6. The maximum temperatures recorded near the aerosol sampling point at the centre location of the bottom, middle, and top elevations are 126 ± 1.0 ºC, 65 ± 0.5 ºC and 59 ± 0.4 ºC respectively. The maximum temperature at off-

centre locations at the 1.2 m elevations was observed to vary between 41 – 46 ± 0.3 ºC. However, there is no significant variation in gas temperature for the other two elevations at off-centre locations.

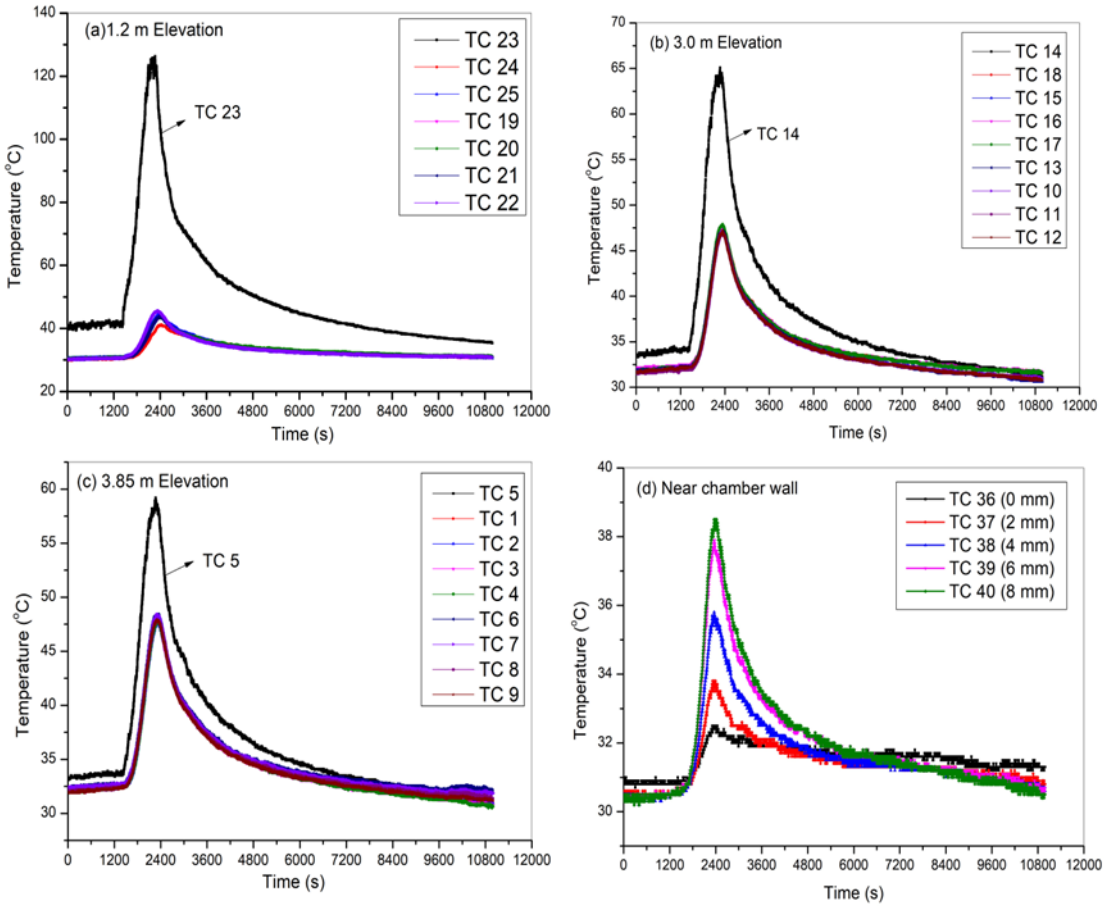

Fig. 6. Evolution of temperature distribution inside the experimental hall at 1.2 m (a), 3.0 m (b) and 3.85 m (c) elevation and near the wall region (d) at the bottom elevation.

The maximum temperature at off-centre locations at the 3.0 m and 3.85 m elevations is ~ 48 ± 0.4 ºC. The maximum difference in temperature between the chamber wall and air at 8.0 mm distance inside the chamber is about 6.0 ± 0.1 ºC (Fig.6 d). The calculated temperature gradient near the wall is 7.5 ± 0.8 ºC/cm. The vertical temperature distribution from the pool surface to the top elevation has a steep gradient from the pool to the region near pool surface, i.e., temperature decreases from 685 ± 5.2 ºC to 200 ± 1.5 ºC at a 0.3 m distance from the pool surface. After that, the temperature drops from 200 ± 1.5 ºC to 59 ± 0.4 ºC, over a 3.40 m distance. The horizontal temperature gradient at the bottom elevation decreases from 126 ± 1.0 ºC to 41 ± 0.3 ºC at a 1.5 m distance from the centre of the chamber. The temperature gradient is higher in the vertical direction than the horizontal due to dominant vertical convection heat transfer. This temperature data is essential for aerosol dispersion and settling behaviour inside the chamber. From the temperature data, the burning duration of sodium pool fire is deduced as ~25 minutes.

A relative humidity (RH) sensor was kept at the bottom elevation and away from the centre region for continuous RH monitoring in the chamber during the experiment. The temporal change of RH% along with gas temperature at the same position is shown in Fig.7. The RH% was observed to reduce from the initial value of 56 ± 0.5 % to 24 ± 0.2 % in 20-min (during pool fire), which may be attributed to the chemical reaction between sodium/ sodium aerosols with moisture and temperature-dependent variation in RH%. The degree of change of moisture saturation also depends on temperature of the air in the chamber. The gradual increase in humidity after 20 min (from T_0) is due to decrease in temperature of the chamber when sodium burning is in quenching stage. The reduction in RH % during combustion and its subsequent increase after the fire was observed to follow the other reported data [18, 19].

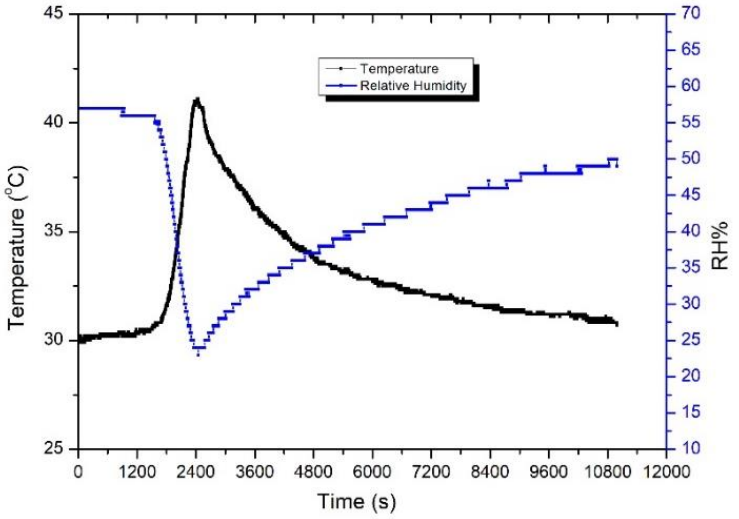

Fig. 7. Evolution of RH% inside the experimental hall at 1.2 m elevation (position 3.10 m x 4.25 m).

3.3. Sodium burning characteristics and aerosol generation rate

After 24 hours of the experiment, a sample was taken from the residue in the tray for determining un-burnt sodium. Post analysis of the residue by hydrogen displacement method reveals that about 10% of sodium was left un-burnt. From the burnt sodium mass and duration of the fire, the average burning, and aerosol release rates are calculated and given in Table 3. The estimated average burning rate of sodium pool and aerosol release rate are 17.3 kg/m^2*hr and 0.24 g/s respectively.

TABLE 3. SODIUM BURING CHARACTERISTICS AND AEROSOL GENERATION.

Experimental parameters	Units	Values
Quantity of sodium used	kg	2.0
Sodium pool area	m^2	0.25
Duration of pool fire	hr	0.42 (25 min)
Quantity of un-burnt sodium	kg	0.2
Quantity of burnt sodium	kg	1.8
Burning rate	kg/m^2*hr	17.28
Aerosol generation rate*	kg/hr	0.86 (0.24 g/s)

*Assume 20 % of the burned sodium manifested as an aerosol.

3.4. Spatial distribution of sodium aerosols concentration

As soon as the sodium burning started, the combustion aerosol was generated and dispersed in the chamber. The mass concentration of sodium combustion aerosol was measured using the filter paper sampling (FPS) method at three elevations and in four locations of each height inside the chamber. The suspended mass concentration of aerosol as a function of time and space is shown in Fig.8. The spatial variation is measured for both horizontal and vertical planes. During the initial period (1st minute) at the centre location, the suspended aerosol concentration is higher in the lowest elevation than in the middle and top; however, for off-centre locations, the concentration at the bottom elevation is lower than the middle and top elevations.

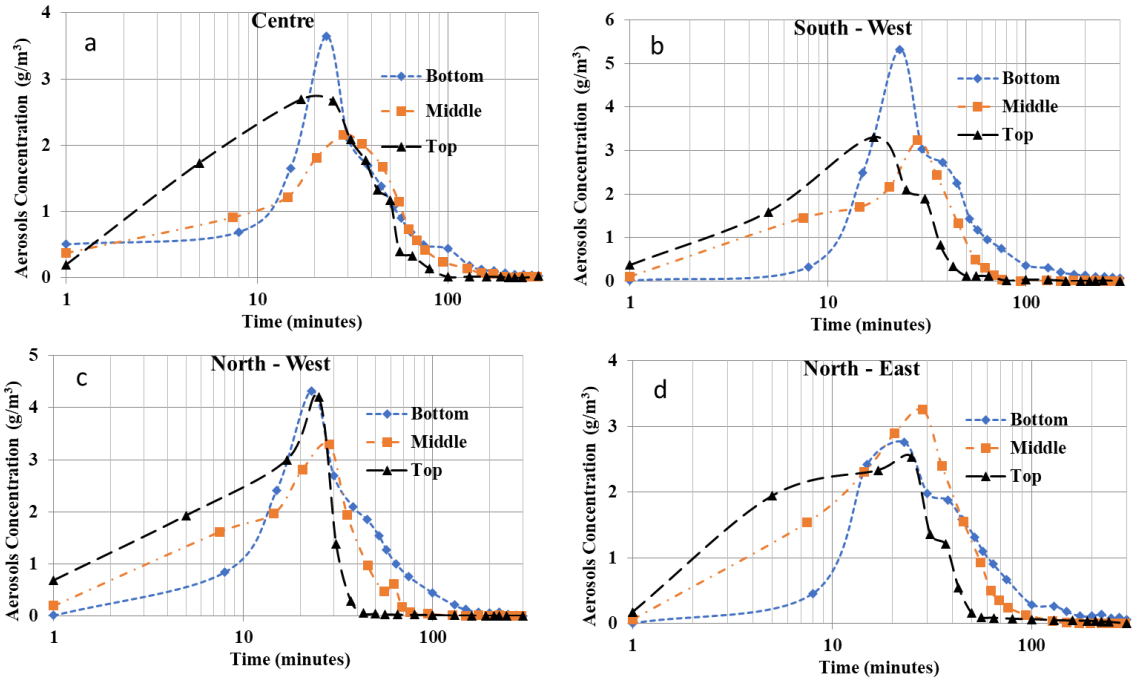

Fig. 8. Vertical distribution of aerosol mass concentration as a function of time inside the experimental hall at the centre (a), South-west (b), North-West (c) and North- east (d) locations.

The suspended aerosol mass concentration at each elevation is found to increase with time initially and reached maximum concentration at ~ 25 minutes and then decreased due to various aerosol deposition processes. During the initial period of combustion (between 10 – 15 min), the average suspended aerosol concentration is higher at top elevation than at middle and bottom. Over time (~ 20 – 25 min), the aerosol concentration at the bottom is more than the top and middle elevations due to settling of the suspended aerosols. The bias in the measured maximum aerosol concentration in the horizontal plane ranges from 2.76 ± 0.11 – 5.32 ± 0.21, 2.16 ± 0.08 – 3.30 ± 0.13 and 2.09 ± 0.08 – 4.21 ± 0.16 g/m^3 for the bottom, middle and to elevations respectively. For the vertical plane, aerosol concentration varies from 2.16 ± 0.08 – 3.65 ± 0.14 g/m^3 for central positions and 2.53 ± 0.10 – 5.32 ± 0.21 g/m^3 for off-centre positions. The measured maximum aerosol concentrations at the bottom, middle and top elevation are 5.32 ± 0.21 g/m^3 (at 23 minutes), 3.30 ± 0.13 g/m^3 (at 28 minutes) and 4.21± 0.16 g/m^3 (at 25 - 28 minutes) respectively. It is observed that the aerosol concentration at the centre location of each elevation is lower than the off-centre locations in a horizontal plane. The average suspended concentration in each elevation shows that the aerosol concentration is higher at the top elevation than at the middle and bottom in the first 20 minutes (aerosol generation period). After cease of the fire, the bottom concentration increased due to settling of the suspended aerosols from higher elevations. Based on the aerosol concentration measurements, it is understood that the aerosol distribution is not well mixed throughout the experimental periods.

3.5. Sodium aerosol size distribution

The size distribution of sodium combustion aerosol was measured by using a low-pressure impactor and aerosol spectrometer. The log-normal aerosol size distribution as a function of time at the bottom elevation is shown in Fig. 9. The higher fraction of particles is formed in the sub-micron size (< 0.5 µm) at the start of the experiment with single-mode, and with the progress of time, aerosols size distribution became multi-mode characterized by a dominant peak in the sub-micron region (< 0.5 µm) and a small peak in the range of 0.57 – 1.26 µm, 1.26 – 4.47 µm and few particles also found greater than 5.0 µm. The number concentration increased from 10^8 - 10^9 /m^3 up to 9 minutes. However, the instrument was unable to record data throughout the experiment due to saturation of the particle counts (maximum count limit ~ 10^9 #/m^3). The growth of aerosol size (multi-mode) may be attributed to progressive sub-micrometre aerosol generation and coagulation with time. Data obtained from LPI (bottom elevation) revealed a multi-mode and polydisperse mass size distribution of sodium aerosol for two samplings time (20 and 60 min). During the initial period, the aerosol size ranged from 0.1 µm to

25 µm with five modes (0.15, 0.75, 1.65, 6.0 and 19.0 µm), and at a later stage, samples have four size modes (0.35, 1.25, 6.0 and 19.0 µm). Overall, the aerosol generated during the sodium pool fire varied in three orders in size and ranges from 0.1 µm to 25 µm.

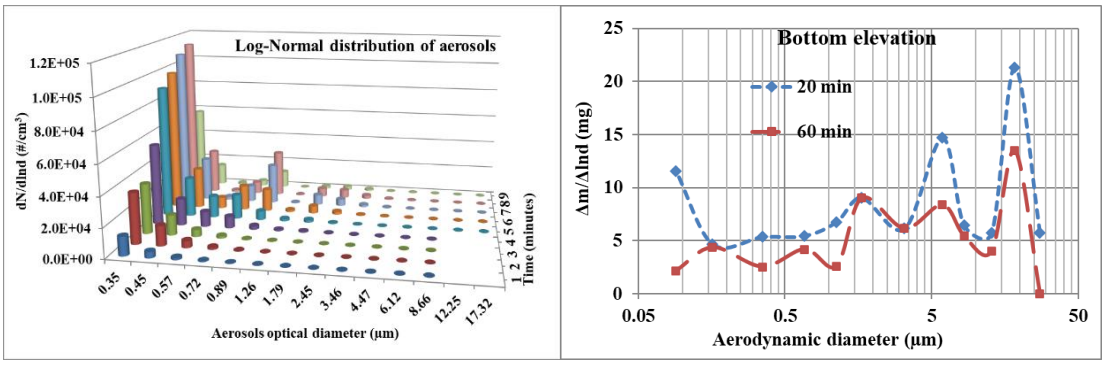

Fig. 9. Log – normal size distribution based on the number (left) and mass (right) as a function of time.

3.6. Aerosol mass deposition velocity

Turntable equipment was used to determine the aerosol mass flux (J) and mass deposition velocity (V_{dep}). The turntable is placed on the chamber floor 35 cm away from the North-East wall. The deposited aerosol sample was collected on the glass plates at regular intervals to determine J. The effective area of each glass plate exposed to the aerosol is 4.5 cm^2 and the exposure duration is 300 s for each plate. For one rotation of the turntable with 16 cups, the total time taken is ~75 minutes. The last plate was not considered for result calculation as it was exposed for ~ 24 hours. The mass of deposited aerosol in each glass plate was determined by the gravimetric method and the deposited mass flux was calculated. The deposition velocities were estimated by using the formula given below:

$$V_{dep.}(\mathrm{m/s}) = \frac{J\ (g/m^2 * s)}{C\ (g/m^3)}, \qquad (1)$$

Where C is the aerosol mass concentration at the respective location at 1.2 m elevation. The aerosol mass deposition velocity and the corresponding fitted aerosol mass concentration measured nearby are plotted in Fig.10. The concentration of sodium aerosol was observed to be gradually increasing during the combustion phase and peaked at 25 minutes (4.04 ± 0.16 g/m^3), then gradually decreased due to settling. The initial mass deposition velocity of sodium aerosol is found to be 0.79 cm/s. The higher deposition velocity could be due to the two components i.e., convection velocity generated due to pool fire and gravitation settling velocity. The gradual reduction in the deposition velocity up to 25 minutes could be attributed to the upward aerosol transport due to combustion process and high aerosol concentration, which hinders convection i.e., the convection of gas diminishes and then aerosols settling starts by gravitational force only. The convection is significantly reduced once the burning of the sodium pool is ceased. Once the aerosol generation is stopped, the aerosol deposition velocity ranged from 0.059 ± 0.005 to 0.289 ± 0.025 cm/s as time increases from 25 – 75 min. The lowest deposition velocity for sodium aerosols is 0.06 ± 0.01 cm/s when the aerosol mass concentration is 4.01 g/m^3. Since mass concentration is high, the aerosols undergo various agglomeration and the aerosol size increases, hence the deposition velocity progressively increases. The average deposition velocity is 0.15 ± 0.07 cm/s during 25 – 75 min. As the aerosol settling phenomenon dominates, the mass concentration of aerosol decreases at all locations with a gradually increase in deposition velocities. Correspondingly, gravitational settling of aerosol causes the increment in deposition velocity with time up to 75 minutes (0.29 cm/s). The value is the equivalent in experiments conducted earlier at the ATF, i.e., 1.0 m^3 chamber [17].

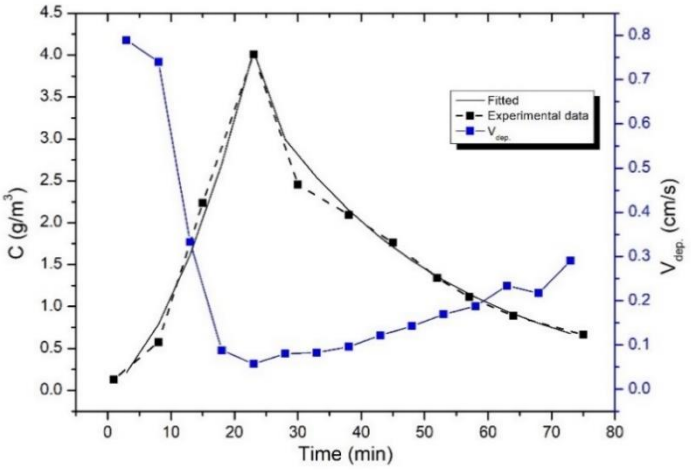

Fig. 10. Aerosol deposition velocity and aerosol concentration as a function of time.

3.7. Distribution of deposited aerosol mass

The distribution of deposited aerosol mass within the surface of the experimental chamber was collected on SS plates (100 cm^2) placed on the vertical and horizontal surfaces. The deposited mass was collected from various locations and dissolved in DM water and then measured using conductometric techniques. Deposited sodium mass is estimated using a pre-established calibration graph [20]. The fraction of total deposited sodium aerosol mass is dominant on the floor (91.96 %) than the side walls (6.70 %) and downward facing surface (1.35%). The aerosol deposited in the horizontal surfaces (floor of the chamber) is dominated by gravitational settling, while vertical surfaces are diffusion and thermophoretic forces.

3.8. Aerosol modelling and comparison with observations

The theoretical model used in the present simulation is based on the first-order differential equations solved by the finite difference method to predict the aerosol characteristics as a function of time in a confined environment. The details of the model description are explained elsewhere [21]. In the present simulation, coagulation due to Brownian motion, coagulation due to polydispersity of aerosol [22], coagulation correction factor for the entire range of particles [23] and aerosol deposition due to gravitational settling, wall plating, thermophoretic and ventilation are considered. Few assumptions are made in the simulation viz., (i) the spatial distribution of aerosol characteristics was not considered, (ii) the gas bulk flow is zero and the particles are homogeneously distributed over the simulation domain, and (iii) the impaction process (which may be significant only at high convection velocities) is neglected. The significant input parameter taken for the estimation of aerosol characteristics is summarized in Table 4. Most of the input parameters were derived from the present experimental results and or taken from literature. The initial aerosol diameter (MMD) and GSD are 0.2 µm and 2.0 respectively and have been taken from measurements.

TABLE 4. INPUT PARAMETERS USED FOR PRESENT SIMULATION.

Experimental parameters	Units	Values
Aerosol source rate	g/s	0.42
Aerosol source duration	s	1500
Mass Median Diameter (MMD)	µm	0.2
Geometric Standard Deviation (GSD)	--	2.0
Density of aerosol	g/cm^3	2.13
Shape factor	--	1.0
Diffusion boundary layer thickness	µm	1.0
Bulk gas temperature	$^\circ$C	50
Chamber wall temperature	$^\circ$C	31
Temperature gradient between gas and wall	$^\circ$C/cm	7.5

The measured and predicted sodium aerosol characteristics (aerosol concentration and median size) as a function of time are given in Fig. 11. The measured maximum average (of four sampling locations in each elevation) suspended aerosol concentration at the bottom, middle and top elevation is 4.01 ± 1.08, 2.98 ± 0.55 and 2.87 ± 0.92 g/m^3, respectively, at ~25 min. The maximum airborne mass concentration reached the different times, as the sample collection time is not the same. The maximum suspended aerosol concentration is higher at top elevation than the middle and bottom (up to 10 minutes); however, after aerosol generation stopped (after 30 minutes), the concentration decreased more rapidly at the top elevation than at middle and bottom. After about 100 minutes, the aerosol concentration decays ~ 90%, 96% and 98% of maximum suspended concentration at the top, middle and bottom elevation, respectively.

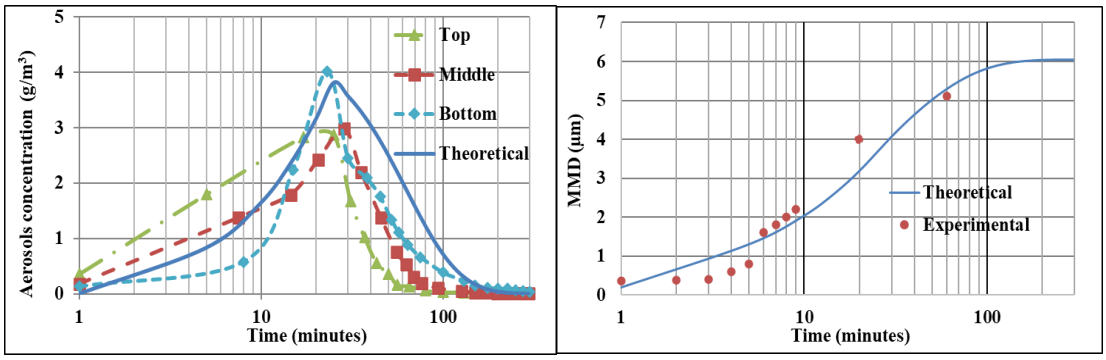

Fig. 11. Evolution of aerosol concentration (left figure) and median size growth (right figure).

The evolutions of aerosol mass concentration by theoretical simulation capture the overall trend, but notably deviated from the data in specific values. However, the predicted concentration reached maxima at 25 minutes, because the source rate is up to that time only. The predicated aerosol concentration for 10 minutes is over-predicted for the bottom elevation and under-predicted for the top and middle elevation concentration. The deviation between the measured and predicted maximum concentration is 5.25%, - 21.79% and - 24.41 % for the bottom and middle and top elevations respectively. At a later stage, the measured aerosol concentration for each elevation decayed faster than predicted. After about 100 minutes, the suspended aerosol concentration is ~ 10%, 4% and 2% of maximum concentration at top, middle and bottom elevation, respectively, while it is 18% as per the prediction.

As shown in Fig. 11, the evolutions of aerosol median size by theoretical simulation capture the overall trend reasonably. The measured aerosol size growth was observed to be slower initially (<5 minutes) than the predicted one. The generated aerosol particles were transported from the source region to other part of the chamber however, in the simulation they are distributed homogeneously. After the 6th min, the prediction and observation size growth matched. The initial aerosol size is 0.2 µm, and the size enlarges one order higher (up to 2 µm) within 10 minutes. Given the large volume of the chamber and presumably highly agitated environment over the particle ejection area, most of the agglomeration has occurred in that zone. After that, the size growth is relatively slower and increased by 5.0 µm in about 60 minutes. In the later stage, the aerosol growth reaches a saturated value when the concentration decay one order less. The growth factor of aerosol size is higher in the initial stage than the later periods due to rapid coagulation at high initial concentrations. However, the effect of hygroscopic growth, turbulent and gravitation agglomeration is not considered in the present simulation. The above parameters will also influence the predictions.

4. SUMMARY AND CONCLUSION

A sodium pool fire experiment was conducted in MINA facility, and spatial-temporal variation of aerosol characteristics was measured. The temperature evolution for the sodium pool, above the pool region, various locations in the chamber and wall has been monitored using matrix of thermocouples. The maximum pool and gas temperatures are found to be 685 °C and 126 °C, respectively, and the temperature gradient near the chamber wall is 7.5 °C/cm. The sodium burning rate was estimated to be 17.3 kg/m^2*hr based on the burning time. The

concentration profile was determined in both horizontal and vertical planes. The measured maximum aerosol concentration in the horizontal plane ranges from 2.76 ± 0.11 – 5.32 ± 0.21, 2.16 ± 0.08 – 3.30 ± 0.13 and 2.09 ± 0.08 – 4.21 ± 0.16 g/m^3 for the bottom, middle and top elevations respectively. For the vertical plane, aerosol concentration varied from 2.16 ± 0.08 – 3.65 ± 0.14 g/m^3 for central positions and 2.53 ± 0.10 – 5.32 ± 0.21 g/m^3 for off-center positions. The maximum average suspended aerosol concentration at the bottom, middle and top elevation is 4.01 ± 1.08, 2.42 ± 0.52 and 2.87 ± 0.92 g/m^3. The aerosol concentration was observed to increase with time till the self-extinguishment of pool fire, then decreased exponentially by various aerosols deposition processes. After 100 minutes, decay in the suspended aerosols concentration is ~ 90%, 96% and 98% for top, middle and bottom elevations respectively. The measured aerosol mass deposition velocity was found to increase from 0.059 ± 0.005 to 0.289 ± 0.025 with an average of 0.15 ± 0.07 cm/s. The size of sodium aerosols analysed from impaction and scattering-based equipment reveals a multi-mode and polydisperse aerosol size distribution. The higher fraction of particles formed in the sub-micron size (< 0.5 μm) at start of the experiment with single-mode, and with the progress of time, aerosols are multi-mode characterized by a dominant peak in the sub-micron region (< 0.5 μm) and a small peak in the range of 0.57 – 1.26 μm, 1.26 – 4.47 μm and few particles also found greater than 5.0 μm. The measured number-size distribution of aerosols by the aerosol spectrometer is multi-mode and ranges from 0.1 – 17 μm. The sodium aerosol diameter ranges from 0.1 - 25 μm, measured by the impaction principle. About 92 % of aerosol is deposited on the bottom floor of the chamber, and the remaining aerosol is deposited on the chamber walls and downward-facing surfaces. A zero-dimensional model predicts the overall trend of evolutions of aerosol mass concentration but notably deviated from the data in all specific values. The evolutions of aerosol median size by theoretical simulation capture the overall trend reasonably.

The present experimental study has given significant insight into understanding the heterogeneous distribution of aerosols along with temperature distribution in closed containment. The results showed that the sodium aerosols size distribution has a wide range (four order variation) for the entire experiment duration. Stratification as well as heterogeneity in the aerosol concentration was noticed in both horizontal and vertical planes in the present experiment. A significant difference was also observed between estimation and observations based on a zero-dimensional model. Hence, the zero-dimensional numerical model may not capture the overall aerosol dynamics in a large containment. The experimental observation can be used for the validation of sodium fire codes and to study aerosol dynamics towards dispersion inside the containment and followed by deposition to increase the confidence in the predictions of EST. Inclusion of aerosol generation models and multi-component distributed aerosol modelling is being initiated.

5. FUTURE DIRECTIONS

The experience gained from the experiment will be used to improve the methodology and instrumentation for capturing the thermal-driven turbulent phenomenon. The sodium fire dynamics, including aerosols behaviour, chemical kinetics and thermal hydraulics are challenging problems that can be addressed with three-dimensional computational fluid dynamics or fire dynamics codes, which will be taken up.

ACKNOWLEDGEMENTS

The authors thank Director, IGCAR for his encouragement and support for conducting this work. The authors wish to acknowledge Mr T. Lokesh and Mr S.S. Ramesh of SED for the erection of sampling lines/ sensors and pressure testing of the test chamber. The authors thank Miss Hyma Kumari for sodium handling, loading and post-experimental cleaning. The authors would like to acknowledge Ms B. Malarvizhi, Mr S.S. Murthy and Mr Avinash Aacharya for providing the heating control, instrumentation, and data acquisition systems. The authors also would like to thank Mr M. Kumaresan for optical video imaging.

REFERENCES

[1] PATEL, P.R., JOHN ARUL, A., In-vessel source term calculation using chemical equilibrium approach for a medium-sized sodium-cooled fast reactor, Nucl. Eng. Des., **362** (2020), 110583.

[2] BASKARAN, R., SUBRAMANIAN, V., VENKATRAMAN, B., Sodium aerosol studies for fast reactor safety, Energy Procedia,**7** (2011), 660-665.
[3] KUMAR, A., SUBRAMANIAN, V., BASKARAN, R., Size evolution of sodium combustion aerosol with various RH%, Aero. Air Qua. Res., **15** (2015), 2270 -2276.
[4] NARAYANAM, S.P., KUMAR A., Sen S., Experimental measurements, and theoretical simulation of sodium combustion aerosol leakage through capillaries, Prog. Nucl. Energy, 118 (2020), 103111.
[5] SANO, T., Y. ABE, T. KIYOKAWA, Experimental studies on sodium columnar fire and pool fire, Proceedings of the LMFBR safety topical meeting, 1982.
[6] CHERDRON, W., JORDAN S., The sodium fire tests performed in the FAUNA facility on up to 12m^2 fire areas. No. KFK--3041. Kernforschungszentrum Karlsruhe GmbH, Germany, 1983.
[7] HILLIARD, R.K., MCCORMACK, J.D., POSTMA, A.K., Aerosol behavior during sodium pool fires in a large vessel: CSTF tests AB1 and AB2, No. HEDL-TME-79-28. Hanford Engineering Development Lab., Richland, WA (USA), 1979.
[8] KUBO, S., HASHIGUCHI Y., OKABE A., R and D needs for evaluation of sodium fire consequences and aerosol behavior for DFBR, 1996.
[9] SOPHY, Y. M., ROY, D., BENTZ, A., The ESMERALDA project for studying extensive sodium fire, No. CEA-CONF-5153. CEA Centre d'EtudesNucleaires de Cadarache, 1979.
[10] JONAS, R., & BUNZ, H., Aerosol behaviour calculations performed with the CONTAIN code in comparison to PARDISEKO calculations and to experiments, J. Aero. Sci., 18, (1987), 935-938.
[11] DUNBAR, I. H., J. FERMANDJIAN, H. BUNZ, Comparison of sodium aerosol codes,1984.
[12] HERRANZ, L.E., LEBEL, L., MASCARI, F., Progress in modeling in-containment source term with ASTEC-Na, Ann. Nucl. Energy**, 112** (2018), 84 - 93.
[13] BANDINI, G., EDERLI, S., PEREZ-MARTIN, S., ASTEC-Na code: Thermal-hydraulic model validation and benchmarking with other codes, Ann. Nucl. Energy**, 119** (2018), 427-439.
[14] NARAYANAM, S.P. KUMAR A., USHA P., Theoretical simulation on evolution of suspended sodium combustion aerosols characteristics in a closed chamber, Nucl. Eng. Technol., **54,** (2022), 2077-2083.
[15] BALDEV RAJ, CHELLAPANDI, P., VASUDEVA RAO, P.R., Sodium Fast Reactors with Closed Fuel Cycle. Sodium fast reactors with closed fuel cycle. CRC press, 2015.
[16] KUMAR A., Sodium Metal Aerosol Characterization in Cover Gas Region, PhD thesis, https://shodhganga.inflibnet.ac.in/handle/10603/274246.
[17] MISRA, J., SUBRAMANIAN, V., KUMAR, A., Investigation of Aerosol Mass and Number Deposition Velocity in a Closed Chamber, Aero. Air Qua. Res., **13** 2 (2013) 680-688.
[18] SUBRAMANIAN, V., KUMAR A., SRINIVAS, C. V., Studies on chemical behavior of sodium fire aerosol in closed and open environment, In Proceeding of IASTA, (2018), 503-508.
[19] SUNDARARAJAN, A.R., MITRAGOTRI, D.S., RAO, S.R.M., Effect of Relative Humidity on Growth of Sodium Oxide Aerosols, J. Nucl. Sci. Technol., 19 (1982), 151-157.
[20] KUMAR, A. SUBRAMANIAN, V., BASKARAN, R., Development and Validation of a Methodology for Characterization of Sodium Aerosols in Cover Gas Region, Aero. Air Qua. Res., **14** (2014), 1534-1541
[21] KUMAR, A., SUBRAMANIAN, V., KRISHNAKUMAR, S., Characterisation of Sodium Aerosol in Cover Gas Region of SILVERINA Loop, Aero. Air Qua. Res., **15** (2015) 1813-1822.
[22] LEE, K.W., & CHEN, H., Coagulation Rate of Polydisperse Particles, Aerosol Sci. Technol., 3 (1984) 327-334.
[23] SHON, S.N., KASPER, G., SHAW, D.T., An experimental study of Brownian coagulation in the transition regime, J. Colloid Interface Sci., 73 (1980) 233-243.